Dilution of Buoyant Surface Plumes

Larsen, Torben; Petersen, Ole

Publication date:
1987

Document Version
Accepted author manuscript, peer reviewed version

DILUTION OF BUOYANT SURFACE PLUMES

by

Ole Petersen
and
Torben Larsen

Department of Civil Engineering
Aalborg University
Sohngaardsholmsvej 57
DK-9000 Aalborg, Denmark

November 1987

List of symbols

U_s	m/s	surface flow velocity cm/s
U_f	m/s	bottom friction velocity $=\sqrt{\frac{\tau}{\rho}}$
ΔT_o	^oC	temperature difference between outlet and flume
T_a	^oC	ambient temperature
T_u	^oC	outlet temperature
z	m	vertical coordinate
x	m	stream wise coordinate
y	m	transverse coordinate
k	mm	equivalent roughness
d	m	water depth
ν	m^2/s	viscosity of water at 20^oC $1 \cdot 10^{-6}$ m^2/s
V	m/s	bulk flow velocity
D_y	m^2/s	transverse bulk diffusion coefficient of plume
D_z	m^2/s	vertical bulk diffusion coefficient of plume
ν_T	m^2/s	eddy viscosity
σ_z^2	m^2/s	vertical spatial variance
σ_y^2	m^2/s	transverse spatial variance
h	m	height
b	m	width
t	sec	time
β		dimensionless tranverse diffusion coefficient
R	m	hydraulic radius
c	kg/m^3	concentration
Q_n	m^3/s	outlet flow
A_n	m^2	outlet area

c_p		specific heat capacity
K	sec	time constant of thermo-couple
ρ	kg/m^3	density
ρ_o	kg/m^3	ambient density
$\Delta\rho$	kg/m^3	$\rho - \rho_o$
M_y^n		nth moment of density distribution around centerline
M_z^n		nth moment of density distribution around water surface
M_T^n		nth moment of temperature distribution
h_o	m	height of outlet
b_o	m	width of outlet
$\overline{\Delta T}$	^oC	mean temperature difference
R		Reynolds number
g	m/s^2	acceleration of gravity

CONTENTS

1. Introduction

Sewage from treatment plants, located at marine recipients, is often discharged through a sea outfall.

A common design criterion for outfalls is that the concentration of E.coli does not exceed 100 coli/ml in more than 5% of the time, in some specific distance from the outfall.

In designing sea outfalls it is therefore essential to be able to predict the dilution and the spatial development of the sewage plume.

Due to differences in salinity and temperature there often are differences in density between the recipient and the sewage.

Previous work by /Weil, 1973. Schrøder, 1980/ have shown that even small density differences strongly affect the behaviour of the plume as it tends to be wide and thin.

The purpose of the present work is to establish a quantitative description of a surface plume which is valid for the range of density differences occurring in relation to sewage outfalls.

This report is devided into two parts.

The first part deals with an experimental investigation of the surface plume.

The second part is an integral description of surface plumes, based on the experiments.

2. Experiments

2.1 Experimental programme

In the experiments the buoyant surface plume is obtained by discharging heated water through an outlet arrangement to the surface in a hydraulic flume.
To avoid jet entrainment, the flow velocity in the flume and outlet velocity are set to equal.

The fundamental measured parameter is the spatial distribution of density differences in subsequent cross sections of the plume.

As independent variables is chosen the outlet temperature difference, ΔT_o, the flow velocity in the flume, u, and bottom friction in the flume, u/u_f.

The transverse and vertical diffusion of the plume, in case of no density difference, is measured separately.

As an illustration of the experimental range are on Figs. 2.1a, 2.1b, and 2.1c shown three pictures recorded by an infra-red sensitive camera. The grey scales correspond to surface temperatures.

The experimental conditions on Fig. 2.1a are high temperature difference and low turbulence level, while Fig. 2.1c corresponds to low temperature and high turbulence level.

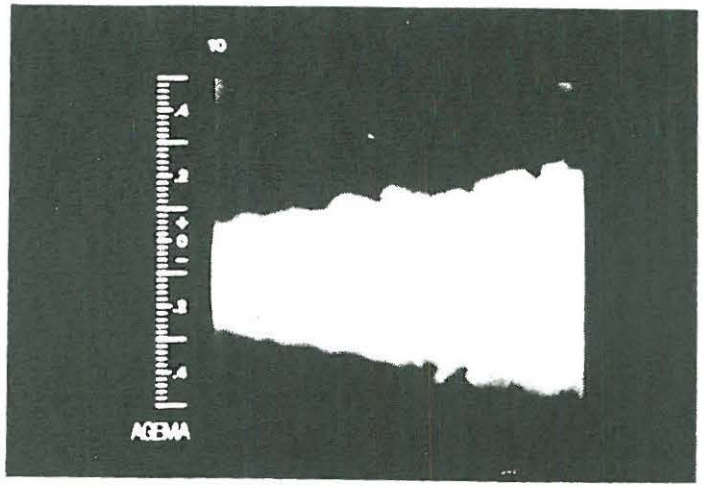

Experiment no. 11

Fig. 2.1.a

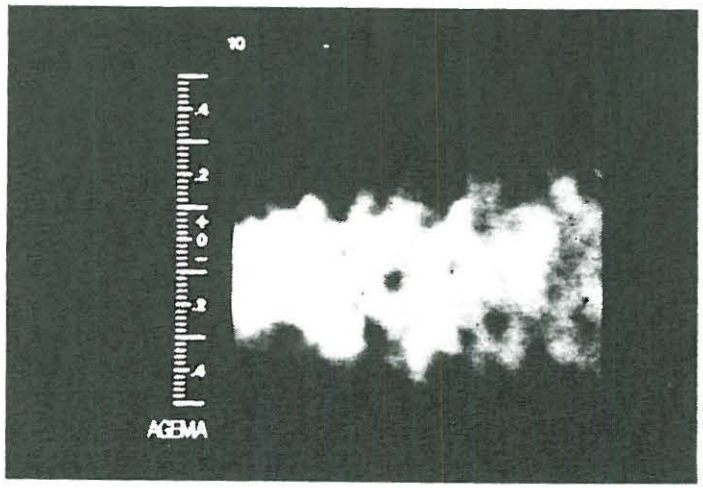

Experiment no. 2

Fig. 2.1.b

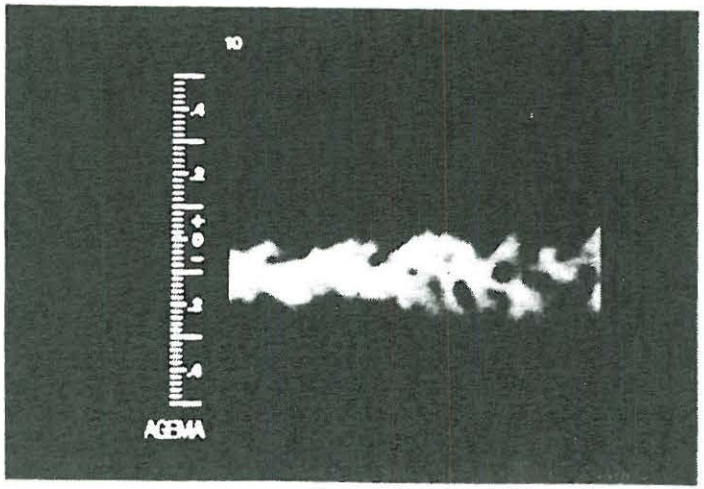

Experiment no. 15

Fig. 2.1.c

In Fig. 2.2 is shown the experimental conditions used in each experiment.

No.	Us [cm/s]	Bottom roughness	Uf [cm/s]	dT0 [Dgr.C]	dRo0 [kg/m3]	Ta [Dgr.C]
1	5.30	2.	0.48	23.4	7.749	22.1
2	5.30	2.	0.48	10.3	2.870	22.3
3	5.30	2.	0.48	3.8	0.953	22.5
4	5.10	1.	0.28	24.2	7.928	21.3
5	5.10	1.	0.28	8.5	2.244	21.6
6	5.10	1.	0.28	2.6	0.615	21.6
7	5.10	1.	0.28	22.1	7.168	21.9
8	9.20	2.	0.84	25.7	8.462	20.8
9	10.20	2.	0.93	10.3	2.766	21.2
10	10.20	2.	0.93	4.6	1.113	21.2
11	10.20	1.	0.53	25.8	7.869	20.6
12	10.20	1.	0.53	12.4	3.376	20.6
13	10.20	1.	0.53	4.6	1.108	21.1
14	15.20	2.	1.38	24.6	7.848	20.1
15	15.20	2.	1.38	12.4	3.318	20.1
16	15.20	2.	1.38	7.2	1.802	20.8
17	15.20	1.	0.77	18.4	5.403	20.1
18	15.20	1.	0.77	9.0	2.268	20.1
19	15.20	1.	0.77	4.6	1.062	20.1
20	15.20	1.	0.77	25.9	8.417	20.1
21	16.60	1.	0.84	5.5	1.316	20.5
22	16.60	1.	0.84	4.0	0.928	20.5
23	15.00	1.	0.76	11.6	3.203	20.7
24	15.00	1.	0.76	5.0	1.229	20.9
25	15.00	1.	0.76	8.8	2.302	21.2
26	15.00	1.	0.76	25.0	8.206	21.0
27	15.00	1.	0.76	13.8	3.918	21.2
28	15.00	1.	0.76	23.7	7.516	20.3
29	15.00	1.	0.76	22.7	7.108	20.5
30	15.00	1.	0.76	24.7	7.932	20.3
31	14.00	1.	0.71	24.8	7.974	20.3
32	15.00	1.	0.76	24.5	7.848	20.4

Fig. 2.2. Experimental conditions.

U_s = flow velocity; U_f = friction velocity;

dT0 = initial excess temperature; dRo0 = initial density deficit;

Ta = ambient temperature.

2.2 The undisturbed flow

2.2.1 Measurement of equivalent roughness

To determine the equivalent roughness, k, of the flume bed is measured a vertical velocity profile in the center of the flume.

Velocity is measured by means of an micropropeller, diameter 0.5 cm, and an electronic device which converts the speed of rotation into an electric current, proportional to the flow speed.

For hydraulic rough flow, the following logaritmic profile can be used /Engelund, 1978/

$$\frac{u}{u_f} = 2.45 \cdot \ln\left(\frac{z}{0.03 \cdot k}\right) \qquad (2.1)$$

where u is velocity in distance z above some, yet undetermined level z_o, u_f is friction velocity and k is equivalent sand roughness.

From the measured profile, z_o is determined, using linear regression on 2.1, as the level which gives the best linear dependency.

In Fig. 2.3 is shown the calculated values of k, for each bed type.

Bottom type	z_o cm	V cm/s	u_f cm /s	k cm
1	0	43.0	2.2	0.072
2	0.8	65.9	6.7	4.0

Fig. 2.3 Equivalent roughness. z_o is measured above flume bed. V = bulk velocity.

As a controle of the measurement and the calculations is plotted u/u_f versus z/k in Fig. 2.4 and as can be seen the profiles match the theoretical values.

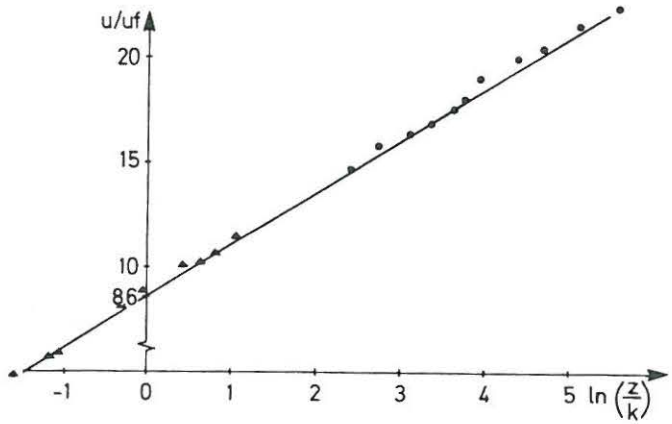

Fig. 2.4 Velocity profiles. ▲ k = 4.0 cm ● k = 0.07 cm

2.2.2 Measurement of undisturbed diffusion coefficients

The diffusion coefficients for the plume in case of no density difference are measured in both vertical and transverse direction, be means of a fluoroscent tracer and an in situ - fluorometer. (Navitronic Fluorometer Q-200).

Transverse diffusion coefficient, D_y

When measuring D_y, the in situ fluorometer is mounted on the transversing waggon, and connected to a digital voltmeter.

The mean concentration, calculated from measurement in app. 10 sec, is measured 1 cm below water surface in 20 equally distributed points across the plume.

From the resulting concentration profile, a plume width is calculated as the mean dispersion around the centroid of the profile.

When the width of the plume σ_y is somewhat greater than the lengthscale of turbulence one can assume that the diffusion coefficient, in a non-dimensional form, is constant /Engelund, 1969/

$$\beta = \frac{1}{2d} \cdot \frac{u}{u_f} \cdot \frac{d\sigma_y^2}{dx} \qquad (2.2)$$

where d = water depth, u = bulk velocity, and u_f = friction velocity.

In Fig. 2.5 is shown the results from the experiments together with the experimental conditions.

No.	U cm/s.	U/Uf	D cm.	X cm.	B cm.	β
1	5.0	18.5	10.0	50.0	2.498	
				75.0	2.874	0.07
				100.0	3.299	0.10
				125.0	3.595	0.08
				150.0	4.667	0.33
				200.0	5.903	0.24
				250.0	7.295	0.34
2	10.0	19.3	10.0	50.0	3.345	
				75.0	3.727	0.10
				100.0	4.300	0.18
				125.0	4.450	0.05
				150.0	4.919	0.17
				200.0	5.257	0.07
3	10.0	11.0	10.0	50.0	3.644	
				75.0	4.055	0.07
				100.0	4.210	0.03
				125.0	5.383	0.25
				150.0	6.081	0.18
				200.0	7.200	0.16
4	15.0	19.8	10.0	50.0	3.380	
				100.0	4.246	0.13
				150.0	4.678	0.08
				200.0	5.522	0.17
				250.0	6.197	0.16
5	5.0	11.0	10.0	50.0	3.140	
				100.0	4.320	0.10
				150.0	5.190	0.09
				200.0	5.923	0.09
6	15.0	11.0	10.0	50.0	2.960	
				100.0	4.208	0.10
				150.0	4.651	0.04
				200.0	5.991	0.16

Fig. 2.5 Transverse diffusion coefficient.

A mean value of β is calculated to

$$\beta = 0.14$$

with standard deviation 0.07.

Compared to other investigations conducted under similar conditions /Engelund, 1969. Fisher, 1979/ this value seems small, but within the range measured under similar conditions.

The vertical diffusion coefficient, D_z.

The vertical diffusion coefficient of the plume is found using a combination of numerical simulation and measurements.

The one-dimensional vertical diffusion equation was solved using a numerical random walk model. For the local eddy viscosity was assumed a parabolic variation with depth. As initial condition was used a gaussian concentration profile.

From the resulting vertical concentration profiles was calculated a height h as the root mean dispersion around the water surface. The vertical diffusion coefficient could then be found as

$$D_z = \frac{1}{2} \cdot \frac{dh^2}{dt} \qquad (2.3)$$

The result from the simulation was a nearly parabolic variation of D_z with depth which could be described as

$$D_z = \gamma \cdot u_f \cdot d \cdot h(1/\sqrt{3} - h/d) \qquad (2.4)$$

The coefficient γ is then determined from experiments.

In the experiments a dilution of Rodamin-B is discharged through the outlet and the vertical distribution is measured in subsequent cross sections.

Water is sampled through 13 siphons, shown on Fig. 2.6, to 1 liter bottles.

Concentration of tracer is measured using the in-situ fluorometer and a 50 ml plexi-glass cuvette.

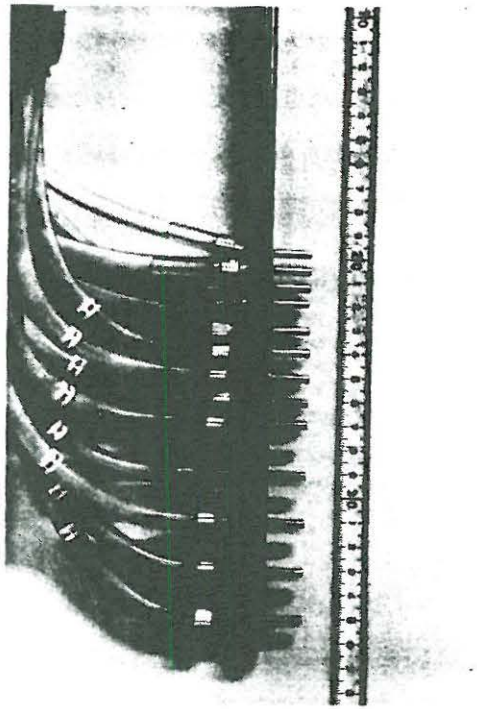

Fig. 2.6

The experiments were conducted using a water depth of 18 cm, flow velocity 10.1 cm/sec. and both roughness types.

In Fig. 2.7 is shown the results from the experiments.

Using (2.3) and (2.4) a value of γ is calculated between each cross section and a mean value of $\gamma = 0.71$ is calculated.

The spread is considerable, but a plot of plume height versus a diffusion distance, as shown in Fig. 2.8, seems to provide a satisfactory fit to the data.

The curve is (2.4) integrated with $\gamma = 0.7$ and an initial height of 1.0 cm.

run	u/u_f	x cm	h cm
1	19	50	1.66
		75	2.00
		100	2.24
		125	2.66
		150	2.89
		175	3.00
		200	3.44
2	19	225	4.06
		275	4.63
		300	5.60
3	11	75	2.48
		100	3.46
		125	3.10
		150	3.74
		175	4.61
		200	5.03
		250	5.80
		300	7.21
4	11	350	8.44
		400	8.48
		375	8.82
		450	8.90
5	11	250	6.21
		300	7.18
		300	7.38
		300	7.66
6	11	200	4.32
		225	4.89
		250	4.87
		275	5.82
		300	7.75
		325	7.95

Fig. 2.7 Measured plume heights.

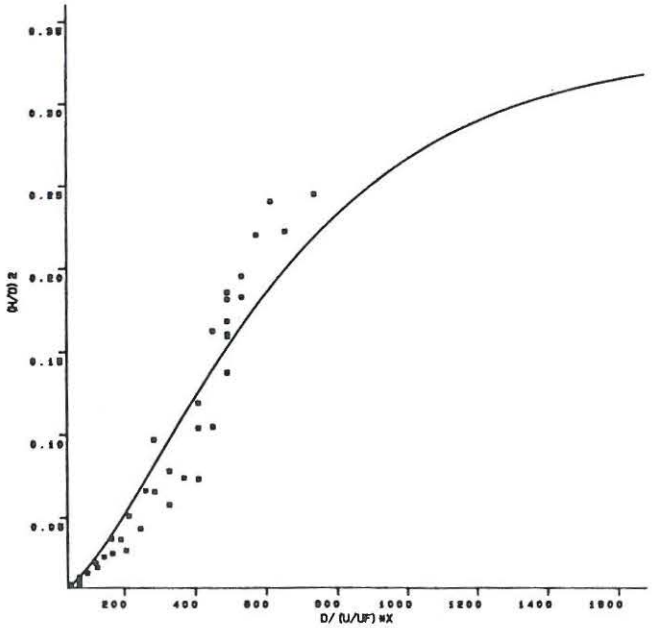

Fig. 2.8 Vertical diffusion coefficient.

2.2.3 Friction velocity

As friction velocity u_f is chosen as scale of the turbulence level in the flow it is essential to determine this for each flow condition used in the experiments.

The velocity measured in each experiment is the approximate surface velocity, u_s measured by means of a floather.

Using Colebrook & White's friction law

$$\frac{V}{u_f} = \frac{2}{f} = 6.4 - 2.45 \cdot \ln\left(\frac{k}{R} + \frac{4.7}{\mathbb{R} \cdot \sqrt{f}}\right) \qquad (2.8)$$

$$\mathbb{R} = \frac{V \cdot R}{\nu} \qquad (2.8a)$$

and a velocity defect law

$$\frac{u_s - V}{u_f} = 2.45 + 2.45 \cdot \ln\left(\frac{d}{R}\right) \qquad (2.9)$$

where R = hydraulic radius, d = water depth, V = bulk flow velocity, k = Nikuradse bottom roughness.

Combining (2.8) and (2.9) the following dependency is derived

$$\frac{u_s}{u_f} = 8.84 - 2.45 \cdot \ln\left(\frac{k}{d} + \frac{3.32}{\mathbb{R}_*}\right) \qquad (2.10)$$

$$\mathbb{R}_* = \frac{u_f \cdot d}{\nu} \qquad (2.10a)$$

from which u_f can be calculated.

2.3 Experiments on plumes

2.3.1 Experimental facility

The experimental facility consists of a 180 ℓ insulated, constant head barrel, which can be filled with water at the desired temperature.

The water flows from the barrel through an adjustable valve and a flow-meter to a deareator, consisting of a closed box where air bubbles can accumulate without influencing the flow.

From the deareator the water is discharged through an outlet arrangement to the surface of the flume.

To prevent shear between the plume and the water in the flume the bulk outlet velocity and the surface velocity on the flume are set to equal.

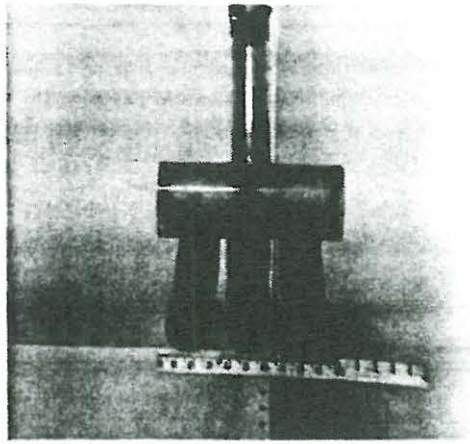

Fig. 2.9 Outlet arrangement.

2.3.2 Temperature measurement

Temperature is measured by means of 8 copper-constantan thermocouples mounted on a metal rod.

The rod is mounted on a transversing waggon, which can be controlled from a computer.

As reference temperature for the thermocouples is used an insulated bottle, mounted on the rod.

The voltage from each thermocouple is amplified 5000 times and registrated on a digital voltmeter, with a smallest increment of 10 mV.

The principle of a thermocouple is that a temperature difference between the two solderings produces a voltage, proportional to the temperature difference.

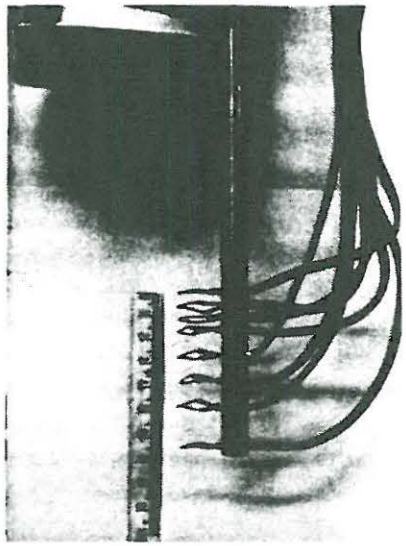

Fig. 2.10 Thermocouples mounting.

The constant of the proportionality for each thermocouple is found by measuring voltage and temperature in a range covering the expected temperatures in the experiments.

The measured parameter in the experiments is temperature difference between plume and ambient water.
Before each traversal the zero of the thermocouples are set to the temperature of the ambient water. This procedure accounts for drift in the electronic equipment and changes in ambient temperature.

Sensitivity of thermocouples are $0.05^{o}C$. Because the temperature fluctuates, it is important to know the time constant of the thermocouples. This has been measured by simulating a temperature step function.

In Fig. 2.11 is shown the registrated temperature as function of time, while the thermocouple is dropped down right in front of the outlet.

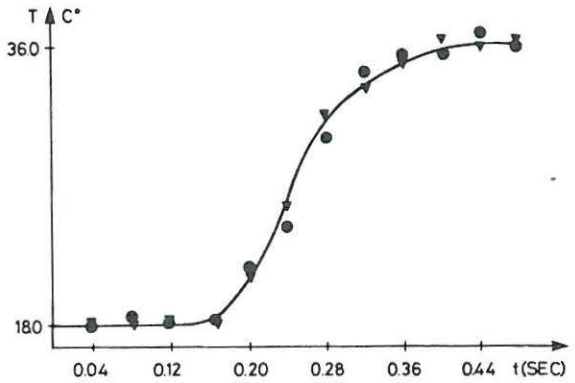

Fig. 2.11 Step response of thermocouple.

Using an energy balance for the soldering one can express the time constant K as

$$T_2 - T = (T_2 - T_1) \cdot e^{-\frac{t}{K}} \qquad (2.11)$$

where T_1 and T_2 are ambient temperature before and after the step, T is the temperature of the soldering, and t is the time.

From the experiment K is found to 0.05 sec.

2.3.3 Temperature to density conversion

As the relationship between the temperature and the density is non-linear, the density differense $\Delta\rho$ is calculated from the measured temperature difference ΔT as

$$\Delta\rho = \rho - \rho_o = f(T_o + \Delta T) - f(T_o) \qquad (2.12)$$

where ρ_o is density of the ambient water, T_o is temperature of ambient water, and f is a functional relationship between density of water and temperature.

The relationship is calculated using quadratic interpolation in a table taken from /Fisher, 1979, Table no. 1/.

When measuring the temperature in the plume the 8 thermocouples are scanned sequentially for 10 seconds in each vertical. Each registrated temperature difference is converted using (2.12) and a mean density difference is calculated for each thermocouple.

2.3.4 Data-reduction and experimental procedure

Each cross section of the plume is divided into 15-20 verticals with equal spacing dependent on plumewidth.

The depth of the rod is adjusted before each experiment, so taht the topmost thermocouple is 0.2 cm below water surface.

The transverse temperatureprofile is approximately normal, while the vertical profile is like a half normal distribution, with top of the water surface.

The resultant two-dimensional density profile is characterized by a vertical, (h), and a horizontal length scale, (b), and a mean density difference, $\overline{\Delta\rho}$.

The length scales are defined by the moments of the distribution

$$M_j^n = \int_{x_i} \int_{x_j} \Delta\rho \cdot x_j^n \, dx_j dx_i \qquad (2.13)$$

where M_j^n is the n'th central moment. Index j refers to axis direction. In vertical direction the distribution is assumed symmetric around the watersurface; $\Delta\rho$ is local time average density difference.

The following definitions appear:

M^o [kg/m] the total mass deficit in the cross section

$h = \left(\frac{M_z^2}{M^o}\right)^{1/2}$ [m] the vertical length scale

$b = \left(\frac{M_y^2}{M^o}\right)^{1/2}$ [m] the horizontal length scale

$\overline{\Delta\rho} = \frac{M^o}{2h \cdot 4b}$ [kg/m³] the mean density difference in the cross section

From this it can be seen that plume width and height equals the standard deviations of the temperature distribution.

The total flux of the excess temperature is used as a controle parameter of the measurement with no heat loss to the atmosphere, conservation of heat equals

$$\Delta T_o \cdot A_o \cdot u = M_T^o \cdot u \qquad (2.14)$$

where ΔT_o is initial temperaturedifference, A_o is area of outlet. Index T refers to substitution of $\Delta\rho$ with ΔT in (2.13)

Rearranging (2.14) yields

$$\frac{M_T^o}{\Delta T_o} = A_o \qquad (2.14a)$$

2.3.5 Results of experiments on plumes

In Fig. 2.12 is shown the main results of the experiments on plumes. For each cross-section is shown the distance from the outlet, the calculated height, width, and mean density difference of the cross-section together with the total temperature difference.

In Fig. 2.13 is shown the ratio of total buoyancy flux to the flux measured as a function of distance from the outlet.

There is apparently some variation, but the scatter seems random.

A linear regression shows no significant trend, which could indicate heat loss to atmosphere.

No.	X [cm]	H [cm]	B [cm]	dRo [kg/m3]	MOt [Dgr.C/cm]
1	50.0	0.705	16.0	0.497	177.800
	100.0	0.799	23.9	0.297	182.200
	150.0	0.968	29.4	0.184	168.400
2	50.0	0.652	9.8	0.412	82.910
	100.0	0.725	16.1	0.216	80.190
	150.0	0.747	21.5	0.135	69.080
3	50.0	1.135	5.4	0.120	23.080
	100.0	0.811	8.6	0.087	18.770
	150.0	0.701	11.9	0.064	16.310
4	50.0	0.582	15.1	0.582	166.500
	100.0	0.704	22.8	0.367	195.300
	150.0	0.663	29.5	0.305	199.300
5	50.0	0.376	9.3	0.654	74.470
	100.0	0.507	14.7	0.308	75.640
	150.0	0.606	21.2	0.181	76.810
6	50.0	1.134	4.3	0.112	17.800
	100.0	0.749	7.3	0.094	16.450
	150.0	0.449	10.0	0.087	12.660
7	50.0	0.600	14.2	0.527	142.700
	100.0	0.734	22.5	0.312	166.600
	150.0	0.617	28.9	0.269	156.200
8	50.0	0.881	7.9	0.956	211.000
	100.0	1.063	14.5	0.418	215.500
	150.0	1.647	19.5	0.201	219.300
9	50.0	1.516	5.4	0.341	92.770
	100.0	1.887	8.9	0.155	85.340
	150.0	1.610	11.8	0.120	74.920
10	50.0	2.031	4.2	0.146	41.840
	100.0	1.864	5.8	0.097	34.580
	150.0	2.723	7.5	0.043	27.520
11	50.0	0.712	9.0	1.188	237.600
	100.0	0.636	15.4	0.799	257.900
	150.0	0.715	21.4	0.481	248.500
12	50.0	0.759	6.1	0.712	111.400
	100.0	0.627	10.5	0.545	122.000
	150.0	0.662	14.8	0.343	115.600
13	50.0	1.338	4.3	0.201	39.110
	100.0	1.232	6.9	0.142	37.460
	150.0	1.029	8.4	0.111	31.770
14	50.0	1.725	4.6	0.786	207.800
	100.0	1.835	7.8	0.398	198.400
	150.0	2.450	10.9	0.213	200.800
15	50.0	2.066	3.5	0.339	87.390
	100.0	2.567	5.5	0.182	91.880
	150.0	2.896	8.4	0.105	89.650
16	50.0	2.208	4.2	0.196	61.640
	100.0	2.669	6.1	0.111	60.400
	150.0	3.022	6.8	0.073	49.760

Fig. 12.a

No.	X [cm]	H [cm]	B [cm]	dRo [kg/m3]	MOt [Dgr.C/cm]
17	50.0	1.015	5.4	0.886	166.200
	100.0	1.055	8.5	0.558	173.000
	150.0	0.904	11.3	0.411	147.900
18	50.0	1.459	3.6	0.371	69.060
	100.0	1.155	6.2	0.343	69.000
	150.0	1.441	7.5	0.147	56.820
19	50.0	1.649	3.6	0.154	32.970
	100.0	1.618	4.8	0.100	27.730
	150.0	1.952	5.9	0.076	30.640
20	50.0	0.869	5.4	1.065	202.900
	100.0	0.643	9.9	0.733	198.100
	150.0	0.701	13.9	0.407	180.300
21	50.0	2.561	2.2	0.068	11.800
	100.0	2.958	3.4	0.040	11.680
	150.0	3.217	5.1	0.025	10.870
22	50.0	1.852	1.7	0.118	12.970
	100.0	2.732	4.2	0.039	13.730
	150.0	2.475	5.2	0.029	11.000
23	100.0	1.547	7.5	0.226	90.950
	200.0	1.503	12.8	0.127	85.280
	300.0	1.720	17.1	0.082	85.620
24	100.0	2.164	6.3	0.081	39.430
	200.0	2.148	8.1	0.058	35.860
	300.0	2.391	12.7	0.036	39.170
25	50.0	1.348	1.9	0.283	25.710
	100.0	1.308	5.4	0.125	31.070
	150.0	1.120	7.0	0.098	27.490
	250.0	1.165	9.9	0.068	27.800
26	50.0	1.271	3.7	0.407	66.560
	100.0	1.399	6.8	0.193	64.750
	300.0	1.825	15.6	0.059	60.770
27	50.0	2.397	4.0	0.135	45.250
	100.0	1.997	5.4	0.112	42.830
	150.0	1.853	7.2	0.084	40.230
	200.0	1.459	7.6	0.080	31.420
	300.0	2.184	10.6	0.040	33.610
28	50.0	1.284	3.2	0.502	73.270
	150.0	1.255	9.1	0.180	75.560
	250.0	1.384	13.2	0.123	82.890
29	50.0	1.349	3.5	0.458	74.840
	100.0	1.222	6.8	0.251	75.320
	300.0	1.560	16.5	0.082	78.520
30	100.0	1.615	6.5	0.185	70.500
	200.0	1.135	10.9	0.137	62.410
	300.0	2.522	16.9	0.056	88.730
31	50.0	1.707	3.9	0.380	88.520
	100.0	1.492	7.0	0.218	82.510
	200.0	1.273	11.2	0.136	71.280
	300.0	1.666	15.8	0.072	70.600
32	50.0	1.308	3.4	0.479	74.260
	100.0	1.262	6.3	0.260	74.400
	200.0	0.945	10.8	0.193	72.410
	300.0	1.774	17.5	0.071	82.180

Fig. 12.b

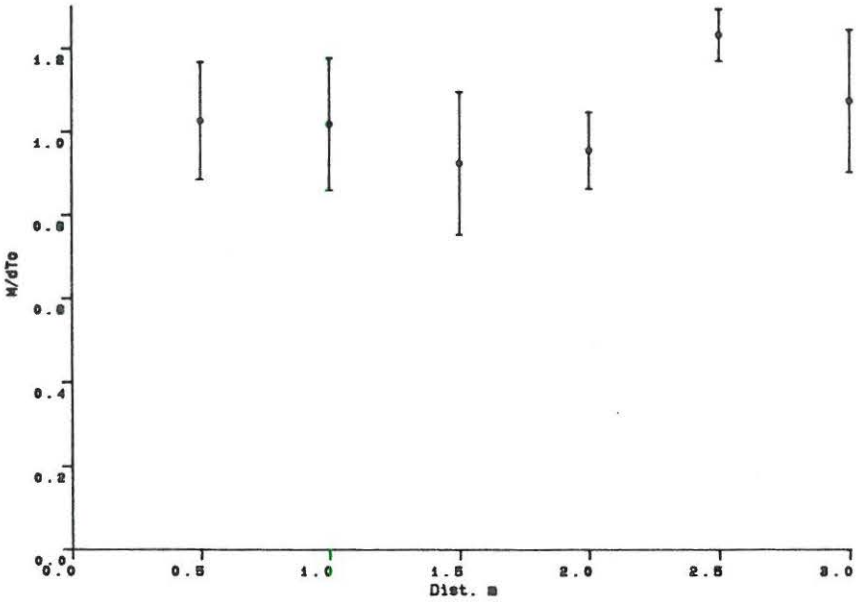

Fig. 2.13 Controle of measurements.

3. INTEGRAL DESCRIPTION OF BUOYANT SURFACE PLUME

The objectives of the integral description is to describe the geometrical development of the surface plume from the transition zone, just after the impingment of the surface, until density differences no longer can be recognized.

In the absence of turbulent energy in the ambient water no mixing will occur, but the buoyancy will spread the plume in a thin surface layer. Eventually some intrainment can be found near the edges of the plume.

When turbulence is present diffusion will occur through the bottom and the sides of the plume.

In the limit with no density differences the mixing will be pure diffusional.

3.1 Initial conditions

In the comparison between the integral description and the measured expansion of the plume between two cross sections, is used measured values in the up-stream cross section as initial conditions.

In practical applications, for example a sewage outfall, the known variables usually are outlet flow, Q_u, density difference between recipient and sewage, $\Delta\rho_u$, and initial dilution, S_o.

Assuming that densimetric Froude number is 1 in the first cross section /Larsen, 1968/, one can derive the following initial values for h and b.

$$b_o = \frac{Q_u \cdot \frac{\Delta\rho_u}{\rho} \cdot g}{4 \cdot u^3} \qquad (3.1)$$

$$h_o = \frac{u^2 \cdot \rho}{2g \cdot \Delta\rho_u} \cdot S_o \qquad (3.2)$$

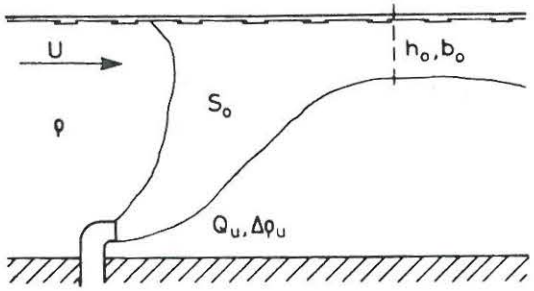

Fig. 3.1 Sea outfall.

3.2 Hypoteses

The plume is described by the plume half width, b, the height of the plume, h, and the mean density difference between the plume and the ambient water, $\Delta\rho$.

In the limiting case of pure diffusional spread with constant diffusion coefficient, the following relation will hold

$$\frac{db}{dx} = \frac{D_y}{u \cdot b} \tag{3.3}$$

$$\frac{dh}{dx} = \frac{D_z}{u \cdot b} \tag{3.4}$$

where h and b, respectively, are defined as the spatial variances of the density distribution. u is ambient flow velocity.

In the case of pure buoyancy spread, the buoyancy induced wavefront will advance at a velocity of

$$v_f \simeq \alpha \frac{u}{\sqrt{g \cdot \frac{\Delta\rho}{\rho_a} \cdot h}} = \alpha \frac{1}{F_d} \tag{3.5}$$

where ρ_a is density of ambient water, g is gravitational acceleration = 9.81 m^2/s and α is a dimensionless number of order one /Weil, 1973/, which is dependent on friction between the two fluids, the h/d ratio, and the actual form of the density profile /Engelund,

1976. Benjamin, 1968/. F_d is a densimetric Froude number defined as

$$F_d = \frac{u}{\sqrt{g \cdot \frac{\Delta\rho}{\rho} \cdot h}}$$

The relation (3.5) is valid only when $u >> v_f$, which is true outside the impingement zone in the sea outfalls.

Defining the total buoyancy as

$$M = h \cdot b \cdot \Delta\rho \tag{3.6}$$

it follows from the conservation of buoyancy that when no mixing occurs

$$\frac{dh}{dx} = -\frac{db}{dx} \cdot \frac{h}{b} \tag{3.7}$$

Assuming that the resultant dispersion of the plume represents the additional influence of diffusion and buoyancy spread it follows from (3.3) and (3.5) that

$$\frac{db}{dx} = \alpha \cdot \frac{1}{F_d} + \frac{D_y}{u \cdot b} \tag{3.8}$$

and using (3.4), (3.5) and (3.6)

$$\frac{dh}{dx} = -\alpha \cdot \frac{1}{F_d} \frac{h}{b} + \frac{D_z}{u \cdot h} \tag{3.9}$$

Previous investigations (fx /Turner, 1973. Schiller, 1975/) show that the presence of density gradients highly affects the turbulence, especially the vertical movements, and thereby affects the turbulent diffusion.

It is assumed that the transverse diffusion remains unaffected. Further it is assumed that the influence on the vertical diffusion relates to a bulk Richordsan R_{io} number as

$$\frac{D_z}{D_{zo}} = (1 + \delta \cdot R_{io})^{-1} \tag{3.10}$$

where D_{zo} is the unaffected vertical diffusioncoefficient, D_z is the

actual diffusion coefficient; δ is an empirical constant, and

$$R_{io} = \frac{g}{\rho}\cdot\frac{\overline{\Delta\rho}\cdot h}{u_f^2} \qquad (3.10a)$$

This dependency is used, although it formally relates the total eddy viscosity to a gradient Richardson number /Munk, 1948/.

Given appropriate initial conditions and values for α and δ the two coupled integral equations can now be solved by using a numerical forward stepping integration technique.

3.3 Comparison with experiments

To give a visual interpretation of the experiments is chosen two plots. The first is based on the observation that the wave front velocity is independent of vertical dilution of the plume.

Based on this (3.8) can be rearranged to a linear form

$$\frac{1}{2d}\frac{u}{u_f}\frac{db^2}{dx} - \frac{D_y}{u\cdot b} = \frac{1}{d}\frac{u}{u_f}\frac{b}{F_d} \qquad (3.11)$$

This relation is shown in Fig. 3.2 and it is seen that the experiments fit eq. (3.11) reasonably well.

For the transverse diffusion coefficient is used the measured values directly.

The second is based on the equation for change in density difference

$$u\cdot\frac{d\Delta\rho}{dx} = -\Delta\rho\cdot\left(\frac{D_y}{b^2} + \frac{D_z}{h^2}\right) \qquad (3.12)$$

Inserting the equation for D_z this yields

$$\frac{D_z}{D_{zo}} = \frac{h^2}{D_{zo}}\left(\frac{u}{\Delta\rho}\frac{d\Delta\rho}{dx} + \frac{D_y}{b^2}\right) = \frac{1}{1 + \delta R_{io}} \qquad (3.13)$$

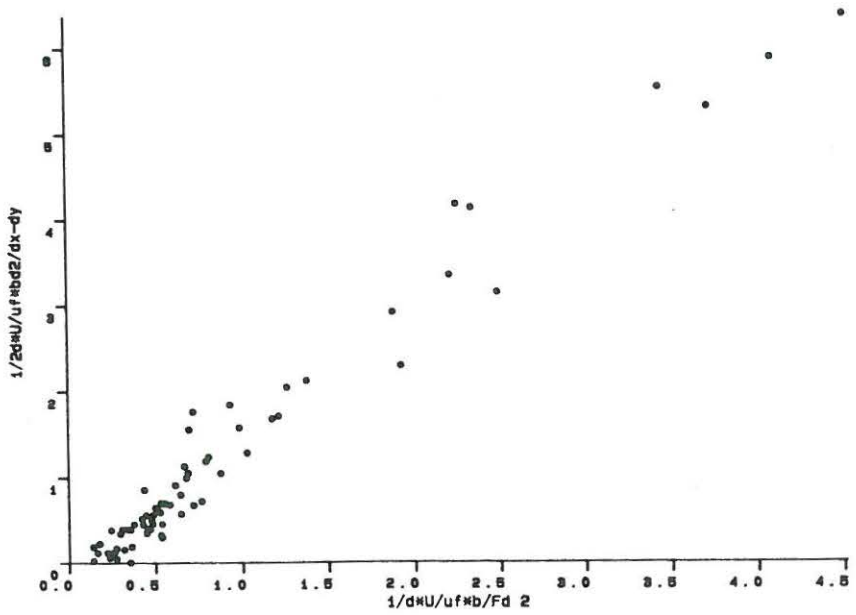

Fig. 3.2 Expansion of plume width.

As shown in Fig. 3.3 one recognizes the hyperbolic dependency, but the scatter is large, which reflects the difficulties in measuring the plume height.

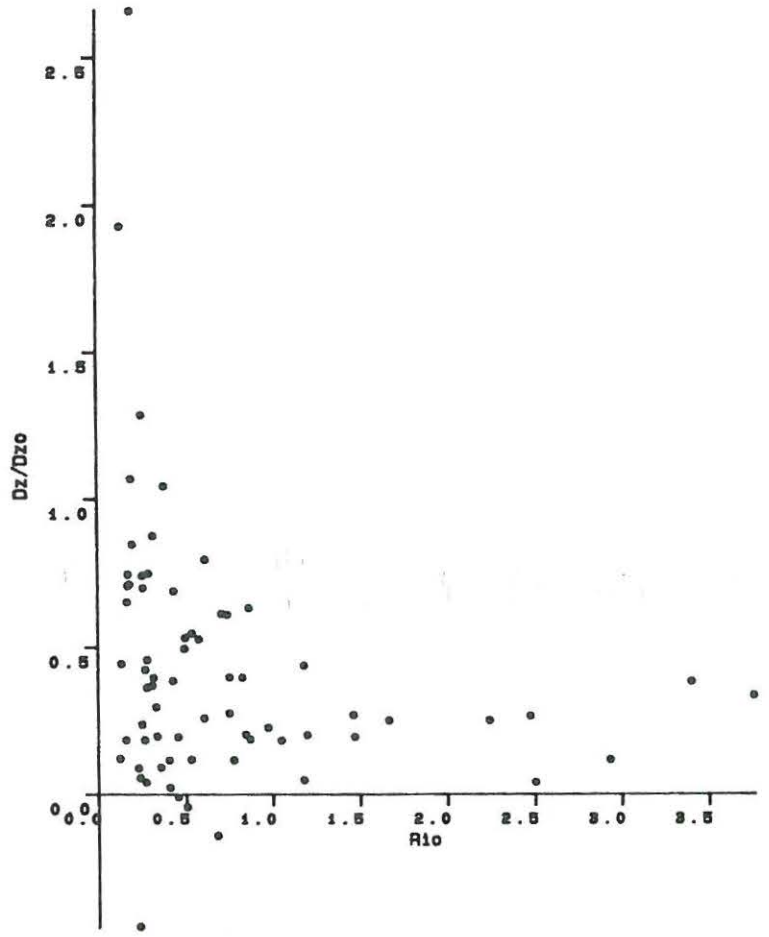

Fig. 3.3 Attenuation of vertical diffusion.

The estimation of the two constants, α and δ, from the experiments could be done from (3.11) and (3.13), but this choise of weighting

will merely be based on the necessity of using a linear dependency, which is a rather arbitrar choise.

One major application of this description is believed to be prediction of concentrations in the near field of sea outfall. Based on this the values of α and δ are estimated to give the best prediction of concentration change, i.e. $\frac{dc}{dx}$.

Using eq. (3.8) and (3.9) and a forward stepping numerical integration, a least-square estimate of predictions compared with experiments can be obtained as

$$0 = \sum_{L=1}^{n} \left(\frac{d\Delta\rho}{dx_c} - \frac{d\Delta\rho}{dx_m} \right)_i^2 \sim \sum_{i=1}^{n} \overline{\Delta\rho} \left[\left(\frac{h_c - h_m}{h_m} \right)_i^2 + \left(\frac{b_c - b_m}{b_m} \right)_i^2 \right] \qquad (3.14)$$

where index c refers to the value obtained from the numerical integration, with the conditions measured in the previous cross-section as initial conditions, index m refers to the measured value and n is the number of plume expansions measured. $\overline{\Delta\rho}$ is a central value of density difference between the two cross sections.

Where it is possible the value of D_y measured under same conditions is used in the integration. Otherwise the calculated mean value is used.

For D_z is used the derived relation (2.5).

Using a gradient based optimization method α and δ are estimated as the value which minimizes the function (3.14).

From this α and δ is estimated to

$$\alpha = 1.35$$
$$\delta = 1.58$$

With these values the distribution of the errors $(\frac{d\Delta\rho}{dx_c} - \frac{d\Delta\rho}{dx_m})$ are shown in Fig. 3.4.

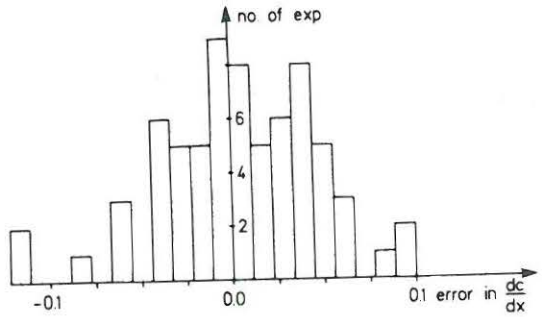

Fig. 3.4 Distribution of errors.

Due to the scatter in the measured variables, α and δ are estimated with some uncertainty. As an analysis of sensitivity to changes on α and δ is on Fig. 3.5 shown a plot of 0 versus respectively α and δ.

The coefficient, γ, which appears in the equation for D_z, has been included in the optimization procedure, and this seems to confirm the value of 0.71.

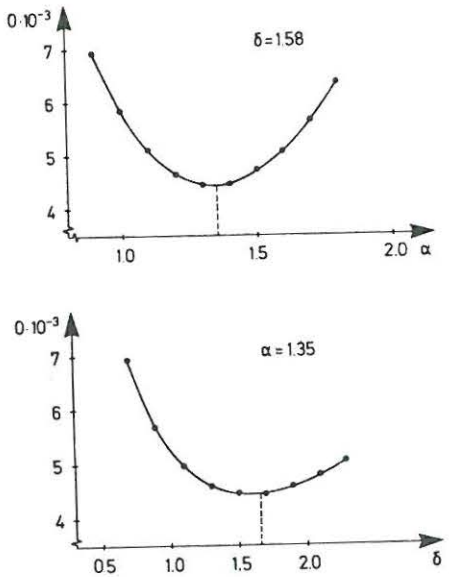

Fig. 3.5 Sensitivity of integral description.

4. DISCUSSION

The purpose of this study has been to establish an appropriate description of the dilution of buoyant surface plumes.

The experiments seem to confirm the hypothesis that the dilution is a result of a buoyancy induced wavefront motion and turbulent diffusion. Further it seems that the description of the attenuation of vertical diffusion is reasonable.

Compared to previous investigations, the coefficient on the buoyant wave front motion seems to be in the correct order of size, though slightly larger than the value found in /Weil, 1979/. This was expected, as the plume width in this study is defined in a depth-integrated manner.

5. SUMMARY

The purpose of the present study has been to establish a description of the dilution of buoyant surface plumes in the near-field of sea-outfalls.

The description is based on two integral length-scales, a local height and width, which charaterize a cross-section of the plume.

The geometrical development of the plume is assumed to be the sum of a buoyant spread, due to the density difference and a turbulent diffusion, where turbulence is generated at the bottom of the ambient water. The density difference is assumed to attenuate vertical diffusion, while the lateral diffusion remains unaffected. At the limit of no density difference, the description has a pure turbulent diffusion as solution.

The two resulting integral equations for the buoyant surface plume are

$$\frac{db}{dx} = \alpha \cdot \frac{\sqrt{g \cdot \frac{\Delta\rho}{\rho} \cdot h}}{U} + \frac{D_y}{U \cdot b}$$

$$\frac{dh}{dx} = -\alpha \cdot \frac{\sqrt{g \cdot \frac{\Delta\rho}{\rho} \cdot h}}{U} \cdot \frac{h}{b} + \frac{D_{zo}}{U \cdot h(1 + \delta \cdot R_{io})}$$

where b and h is a characteristic width and height,
U = ambient velocity, ρ = ambient density,
$\Delta\rho$ = local mean density deficit, D_y = lateral diffusion coefficient
D_{zo} = vertical diffusion coefficient, R_{io} = local bulk Richardson number, and g = acceleration of gravity,
α and δ = constants.

The integral description has been calibrated against a series of laboratory experiments, conducted under varying conditions of density difference and turbulence level. From the calibration the numerical constants has been determined to $\alpha = 1.35$ and $\delta = 1.58$.

6. REFERENCES

Engelund, Frank, 1969:
"Dispersion of floating particles in uniform channel flow"
J. of Hydraulics Div., ASCE vol 95, No HY4.

Engelund, Frank and Pedersen, Fl. Bo, 1978:
"Hydraulik"
Den private Ingeniørfond, Danmarks Tekniske Højskole.

Benjamin, T. Brooke, 1968:
"Gravity currents and related phenomena"
J. of Fluid Mech., vol. 31 part 2, pp 209-248.

Fischer et al., 1979:
"Mixing in Inland and Coastal Waters"
Academic Press.

Larsen, I and Sørensen, T.:
"Buoyancy spread of waste water in coastal regions"
Proceedings, 11th Int. Conf. on Coastal Engineering,
London 1968, pp 1397 - 1402.

Munk, W.H. and Anderson, E.R., 1947:
"Notes on a theory of the thermocline"
J. of Maritime Research, vol. 7, pp 276-295.

Schiller, E.J. and Sayre, W.W., 1975:
"Vertical Temperature Profiles in Open Channel Flow"
J. of the Hydraulics Div. ASCE vol. 101, No. HY6, pp 749-761.

Schrøder, Hans, 1980:
"On the spreading and mixing of buoyant plumes"
Danish Hydraulic Institute.

Weil, J. and Fischer, H.B., 1974:
"Effect of stream Turbulence on Heated Water Plumes"
J. of the Hydraulics Div. ASCE vol. 100, No. HY7, pp 951-970.